SSRG International Journal of Civil Engineering
ISSN: 2348-8352/ https://doi.org/10.14445/23488352/IJCE-V13I4P102

Volume 13 Issue 4, 17-32, April 2026

Original Article

Production of One-Part Alkali-Activated Mortars Reinforced with Waste-Based Corn Stalk Fibers

Kübra Ekiz Barış

Department of Architecture and Design, Kocaeli University, Kocaeli, Türkiye.

Corresponding Author : kubra.ekizbaris@kocaeli.edu.tr

Received: 05 January 2026 Revised: 04 February 2026 Accepted: 03 March 2026 Published: 28 April 2026

Abstract - *The objective of this experimental research is to investigate the possibilities of using waste-based Corn Stalk Fibers (CSF) in one-part Alkali-Activated Mortars (AAMO) to determine the impact of fiber properties on the physical, thermal, and mechanical characteristics of the material and the effectiveness of the fiber in increasing the strength under bending loads and developing ductile fracture behaviour. The optimal fiber content and length are 3% and 30 mm, respectively. Increasing the CSF content from 1% to 3% increases the Flexural Strength (FS) of the AAMO while decreasing its Unit Weight (UW), Compressive Strength (CS), Ultrasound Pulse Velocity (UPV), Modulus of Elasticity (MoE), and Thermal Conductivity coefficient (TC). More ductile fracture behaviour is observed with the inclusion of CSF. The porosity (P) (19.11%), Water Absorption ratio (WA) (14.89%), TC (0.48 W/mK), and FS and CS (3.36 and 6.03 MPa, respectively) of the CSF-reinforced one-part AAMO meet the expected performance criteria. Although extending the curing period from 28 days to 365 days enhances the properties, the period between 28 and 90 days is more effective.*

Keywords - *Alkali activation, Fiber content, Fiber length, One-part mixing method, Waste corn stalk fiber.*

1. Introduction

Approximately 36% of overall energy consumption and 40% of CO_2 emissions connected to energy use are attributed to the construction industry. In particular, Portland cement-based products are responsible for CO_2 emissions because of their extensive use globally [1]. Approximately 8% of greenhouse gas emissions worldwide come from the production of these materials, which adversely impact the environment and contribute to climate change, specifically global warming [2]. As a result, for many years, attempts have been made to develop construction materials with low CO_2 emissions and energy- and resource-efficient substitutes for cement.

The use of additional cementitious materials [3], the reuse of wastes from construction activities [4], and the use of innovative alternative binders without cement, such as geopolymer or Alkali-Activated Materials (AAM), instead of cement [5], can contribute to the reduction of CO_2 emissions. AAM is a binder produced by the activation of raw materials with an aluminosilicate-based internal structure using alkali-based materials at low temperatures below 100 ºC [6]. AAM is described as an improved, environmentally conscious alternative binder compared to cement [7]. This description is provided because AAMs can be produced from various, readily available, waste- or by-product-based raw materials with a lower embodied carbon content compared to traditional cement and require lower energy during production, achieve high strength at low temperatures and early curing periods, and are cost-effective [8]. With the use of AAM, it is determined that CO_2 emissions may be reduced by up to 80% based on the variety of raw resources and the production process [9].

In addition to industrial by-products or waste materials, naturally occurring volcanic-based materials can serve as a source of aluminosilicate (precursor) for the production of AAM because they have a high content of amorphous SiO_2 and Al_2O_3. Research results related to the production of AAM from natural volcanic materials originating from Iran [10-12], Italy [13-15], Cameroon [16-18], Saudi Arabia [19, 20], Jordan [21], Japan [22], China [23], Indonesia [24], Germany [25], and Colombia [26] are promising. In Türkiye, it has been determined that pumice extracted from Hasankale (Erzurum) [27], perlite from Erzincan [28], volcanic ash from Manisa [29], and volcanic tuff from Bayburt [30] are suitable for AAM production. Over 1.5 billion m^3 of volcanic tuff deposits were found in the Cappadocia Region of Türkiye, resulting from the eruptions of historically active volcanoes [31]. Experimental studies in the literature [32, 33] have determined that Nevşehir Pozzolan (NP) can react with various alkaline activators, making it advantageous for the manufacturing of alkali-activated binders, mortars, and concrete.

The properties of AAMs differ based on the type and characteristics of the raw materials, the mixing ratio, and the production and curing conditions. The mixing method is one of the most significant aspects that alter the material properties. Depending on whether the alkali activator used is in a solid or liquid state, there are two different mixing methods: (i) two-part mixing; and (ii) one-part mixing. Those produced using the two-part mixing method are traditional AAMs [10]. In this method, the chemical alkaline activators are prepared 24 hours before the mixture is made, and are added during the mixing process with the aluminosilicate source. However, this method is not an easy one to apply. Dangerous accidents can occur during the use of the activator solution. Preparing activators with abrasive properties to ensure the safety of field workers can limit the mass production capabilities of the material [34]. In AAMs produced using the one-part mixture method, similar to traditional Portland cement, the aluminosilicate source and solid alkali activators are mixed in solid form until a homogeneous mixture is obtained, with the reaction being initiated by adding water when application is intended. This method, which facilitates the processing of dry raw materials, offers easier, safer, and more practical use in large-scale applications [35]. Thus, it offers significant advantages in areas such as traditional mixing, storage, raw material transportation, occupational safety, and compliance with user health, making it more readily accepted by the construction materials market [36, 37]. The mixing method predominantly used in research on the production of AAM using volcanic-based materials is the two-part method. In particular, detailed experimental research is needed for the production of AAMs using the one-part mixing method with the natural volcanic raw materials of Türkiye.

Similar to other binding materials, AAM also exhibits brittle behaviour and suddenly fractures under bending or tensile loads [38]. To address this negative characteristic, fillers or fibers are added to the AAM mixture to produce AAM composites. These composites may include various synthetic fibers, such as polypropylene, polyvinyl alcohol, and polyethylene, as well as glass and carbon fibers. This is because they are very durable and strong, and can greatly improve crack control and behavior after cracking. However, their high cost and adverse effects on the environment have led to the search for alternatives that are more sustainable. Natural fibers are preferred due to their advantages, such as abundance, ease of preparation, non-toxicity, renewability, low cost, and environmental friendliness. They possess a lot of distinctive physical and mechanical characteristics that are influenced by variables such as the type, length, content, and chemical composition of the fibers. The literature indicates that their UW usually ranges from 1.2 to 1.5 g/cm³, and their tensile strength may vary from 120 to 900 MPa. Similarly, the MoE typically ranges between 4.8 and 90 GPa, and the elongation may reach values between approximately 0.59% and 25% [39]. In the literature, sisal [40, 41], coconut [41], hemp [42, 43], cotton [44, 45], jute [46], sugarcane bagasse [47], kenaf [48, 49], flax [50, 51], musa basjoo [52], and wood fibers [53] are the types of natural fibers used in AAM production. Compared with these fibers, corn-based fibers represent an abundant agricultural residue with relatively low UW and acceptable mechanical properties, which may contribute to improving the toughness and crack resistance of binder systems while simultaneously reducing material cost. In addition, the use of CSF can alleviate the challenges of waste disposal caused by maize cultivation. Despite all these advantages, studies on using CSF for producing building materials are limited. Thus, it is essential to fill this gap for both long-term waste management and the production of building materials that have positive effects on the environment.

Corn, among the most extensively transported food products, has an annual production of over 1.2 billion tons worldwide and 6.75 million tons in Türkiye [54]. The waste generated from corn production is generally disposed of in the environment, causing pollution, or is burned, which poses a significant risk to human well-being and the environment [55]. Corn cob waste, especially, can be used in the construction industry as an aggregate in alkali-activated binder, mortar, or concrete mixtures [56, 57], or after being burned, as corn cob ash [57, 58]. However, the use of other parts of corn waste, such as stalks and leaves, in the production of materials is limited. The production of corn fiber from corn stalks and leaves, and the use of CSF reinforcement in binders, are advantageous both in terms of enhancing the properties and environmental sustainability of the produced material.

CSF has been added as reinforcement to traditional Portland cement and hydrated lime mortars [59], coal gangue-filled cementitious binders [60], cement-stabilized compressed earth mixtures [61], lightweight concretes with EPS aggregate [62], and traditional concrete [63], resulting in increased FS and ductility. However, scarce data exist on the effectiveness of CSF, an agricultural waste-based fiber, within AAM. A study [64] produced a metakaolin-based two-part AAM with an FS of 6.7-8.8 MPa after adding 12-14.5% CSF. CSF significantly increased the ductility of the composite material. In the literature, there is no research on the use of CSF in one-part AAMO. Thus, this experimental research proposes to address the current knowledge gap by incorporating waste CSF produced from corn stalks in a one-part AAMO design. A comprehensive evaluation of the effects of CSF content and length on the physical, thermal, and mechanical properties of the produced one-part AAMO was carried out. This study not only makes CSF waste more valuable, but it also helps produce environmentally friendly AAMO. In this context, the current study provides a novel perspective by combining waste CSF with one-part AAM production technology. This approach helps both the production of sustainable materials and the use of resources in a circular way.

2. Methodology

2.1. Raw Materials

The NP aluminosilicate source was acquired from the waste storage site of the volcanic rock quarry in Nevşehir. NP was first dried at 80 ºC for 48 hours and ground to a fineness of less than 90 µm before use. Its specific gravity and specific surface area were 2.55 and 7648 cm^2/g, respectively, as determined according to TS EN 196-6 [65]. Since the total ratio of SiO_2, Al_2O_3, and Fe_2O_3 is greater than 70% (Table 1), NP can be classified as a natural pozzolanic source for binder production and as a low-calcium-content (0.33% CaO) raw material for AAM, according to TS 25. The results for FS (1.86 MPa) and CS (6.81 MPa), respectively, obtained from the pozzolanic activity test, fulfill the criteria of the specification.

Table 1. Chemical constituents of NP

Constituent	NP (%)
SiO_2	77.29
Al_2O_3	18.48
Fe_2O_3	1.71
CaO	0.33
MgO	1.29
K_2O_7	0.30
SO_3	0.10
LoI	0.50

In the AAMO production process, a chemical alkaline activator should be used to raise the pH of the mixture to ensure the dissolution of the raw materials and the subsequent evolution of polycondensation stages [66]. Solid sodium hydroxide (NaOH) and anhydrous sodium metasilicate (SS) containing 50-52% SiO_2, and 50-48% Na_2O were used. The aggregate utilized was standard sand (SK), which had a maximum particle diameter of 2 mm [67]. CSF was obtained from Ordu, and its composition, determined by XRF analysis, includes 55.60% cellulose, 8.70% hemicellulose, 13.80% lignin, 1.60% pectin, and 8.90% waxy components (Table 2).

Table 2. Chemical constituents of CSF

Constituent	CSF (%)
Cellulose	55.60
Hemicellulose	8.70
Lignin	13.80
Pectin	1.60
Wax	8.90
Humidity	11.40

According to the literature data, the UW, FS, and MoE of the CSF are 1.34 g/cm^3, 522.4 MPa, and 17.4 GPa, respectively [59]. When preparing CSF, first, the leaves, ears, and nodes were removed from the surface of the stalk (Figure 1(a)). The inner part of the stalk (core, pith) (Figure 1(b)) was removed, and the remaining rind (skin) (Figure 1(b)) was cut into 10-, 20-, 30-, and 40-mm fiber lengths with sharp scissors (Figure 1(c)). The presence of a waxy layer on the CSF surface can weaken the adhesion between the matrix and CSF. Furthermore, the existence of cellulose, hemicellulose, and lignin in CSF can reduce long-term durability within an alkaline matrix, accelerate fiber degradation, and lead to loss of strength. To increase the durability of CSF and ensure strong adhesion between the matrix and CSF, alkaline treatment is necessary [60, 62]. This treatment may also break down the hydrophilic hydroxyl components [68, 69] and the saccharide components of the fibers that delay the hardening of the binder [70, 71]. Therefore, the CSF was subjected to alkaline treatment (Figure 1(d)). CSF was subjected to an alkaline treatment for 6 hours in a 1% SS solution with a pH of 12. After the alkaline treatment, CSF was washed with water and dried at 50 ºC for 24 hours until a constant weight was reached (Figure 1(e)). The CSF (Figure 1(f)), cooled to room temperature, was kept ready for use in a closed glass container.

2.2. Mixing Ratios

The one-part AAMO without CSF was defined as the control sample (ref). Total alkali activator (NaOH + SS): NP, NaOH: SS, and binder: SK ratios were kept constant by weight at 1:4, 1:2, and 1:3, respectively (Table 3). CSF was incorporated at 1%, 2%, and 3% of the weight of NP. The maximum CSF content (3%) was determined as a result of preliminary trials and constrained by workability to prevent adverse casting situations. After incorporation of CSF, it will absorb the matrix's water, resulting in a decrease in workability. However, adding more water to the mortar to compensate for the reduced workability can further decrease the mechanical properties [40]. Therefore, the optimal amount of water that ensures the workability was figured out via the flow table test [72] (Figure 2(c)), and the water/binder ratio was maintained at 0.65. The maximum CSF length (40 mm) was also determined during the preliminary experiments. During the preparation of the mixture, especially after the addition of water, it was determined that CSF longer than 40 mm tends to clump excessively. To prevent fiber agglomerations within the matrix and the subsequent formation of a heterogeneous AAMO, the maximum CSF length was limited to 40 mm. The produced samples are coded in the format [x/CSF-%y]. In this coding, "x" is the length of the CSF (10, 20, 30, and 40 mm), and "y" is the CSF content in the AAMO (1%, 2%, and 3% by weight of NP).

2.3. Sample Preparation, Curing Conditions, and Applied Tests

NP, SK, NaOH, SS, and CSF were mixed dry for 5 minutes according to the one-part mixture method (Figure 2(a)). The water was then added and mixed for another 5 minutes (Figure 2(b)). Half of the mortar was placed in the 40x40x160 mm molds, and the vibration was carried out for 30 seconds. Then, the remaining part of the mixture was poured into the molds, which were re-vibrated, then covered with polyethylene (PE), and subjected to a pre-curing process at 22 °C for 12 hours. After removing from the molds, the samples were pre-cured for another 12 hours (Figure 2(d)) and subjected to ambient curing for 28 days at 22±2 °C and 50±5% RH without PE coating (Figure 2(e)). Production stages of CSF-reinforced one-part AAMO samples are presented in Figure 3.

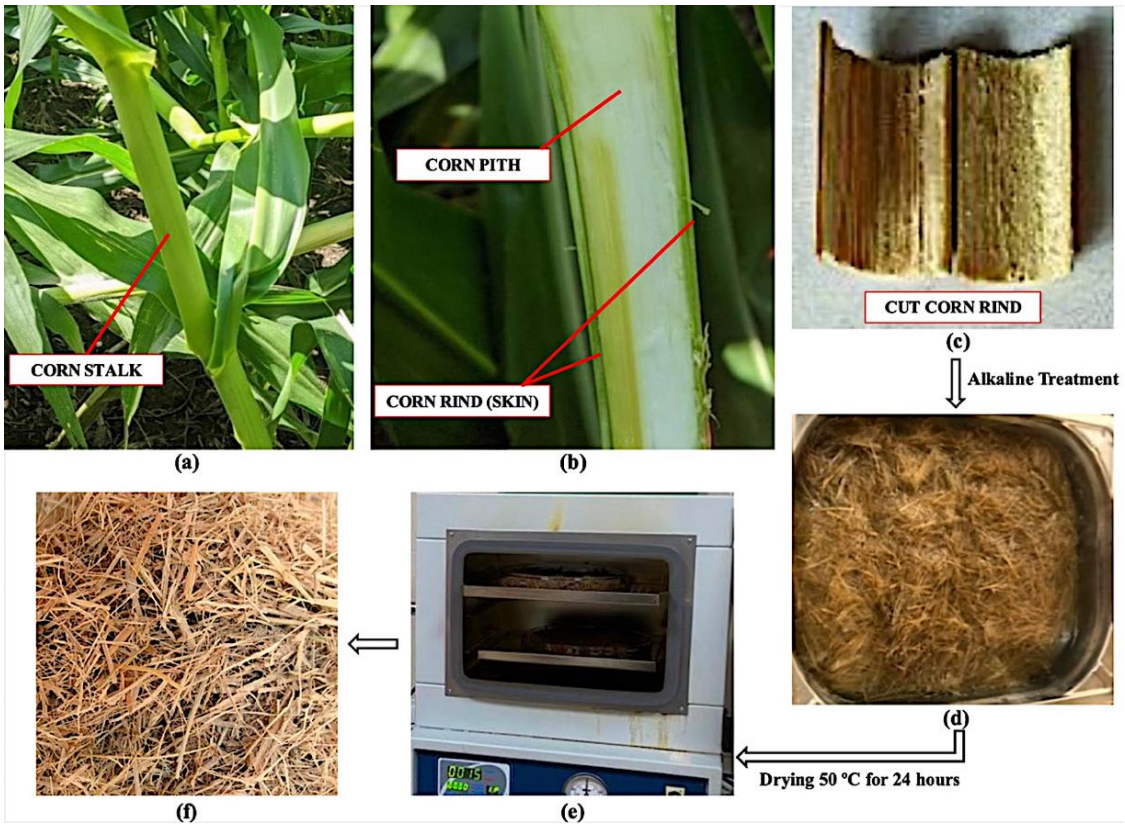

Fig. 1 (a) The stalk of the corn plant, (b) Corn pith and corn rind inside the corn stalk, (c) Corn rind after cutting with a sharp scissor, (d) Alkaline treatment of the corn rind, (e) Drying the corn rind at 50 °C for 24 hours, and (f) CSF ready for use in the AAMO.

Table 3. CSF-reinforced one-part AAMO mixing ratios

Sample	NP (g)	SK (g)	NaOH (g)	SS (g)	CSF (g)	Activator: aluminosilicate	Binder: SK
Ref	400	1200	33.3	66.6	0	1:4	1:3
10/CSF-1%					4		
20/CSF-1%							
30/CSF-1%							
40/CSF-1%							
10/CSF-2%					8		
20/CSF-2%							
30/CSF-2%							
40/CSF-2%							
10/CSF-3%					12		
20/CSF-3%							
30/CSF-3%							
40/CSF-3%							

In the first stage of this research, the influence of CSF content and length on the physical, thermal, and mechanical performance of one-part AAMOs, as specified in Table 3, was examined. After determining the optimal CSF content and length, the influence of the sample's curing period under ambient conditions was examined by extending the 28-day curing period to 60, 90, 180, and 365 days. The efficiency of the curing period was determined only on the samples with the optimal CSF content and length. Except for the TC test, all other experiments were conducted on 6 prismatic samples measuring 40x40x160 mm; the TC test was applied to 6 cylindrical samples having a 100 mm diameter and 10 mm thickness.

Fig. 2 Production of CSF-reinforced one-part AMMO samples: (a) Preparation of dry mix, (b) Fresh AAMO, (c) Flow table test, (d) Pre-curing of the samples, and (e) Samples after the curing period.

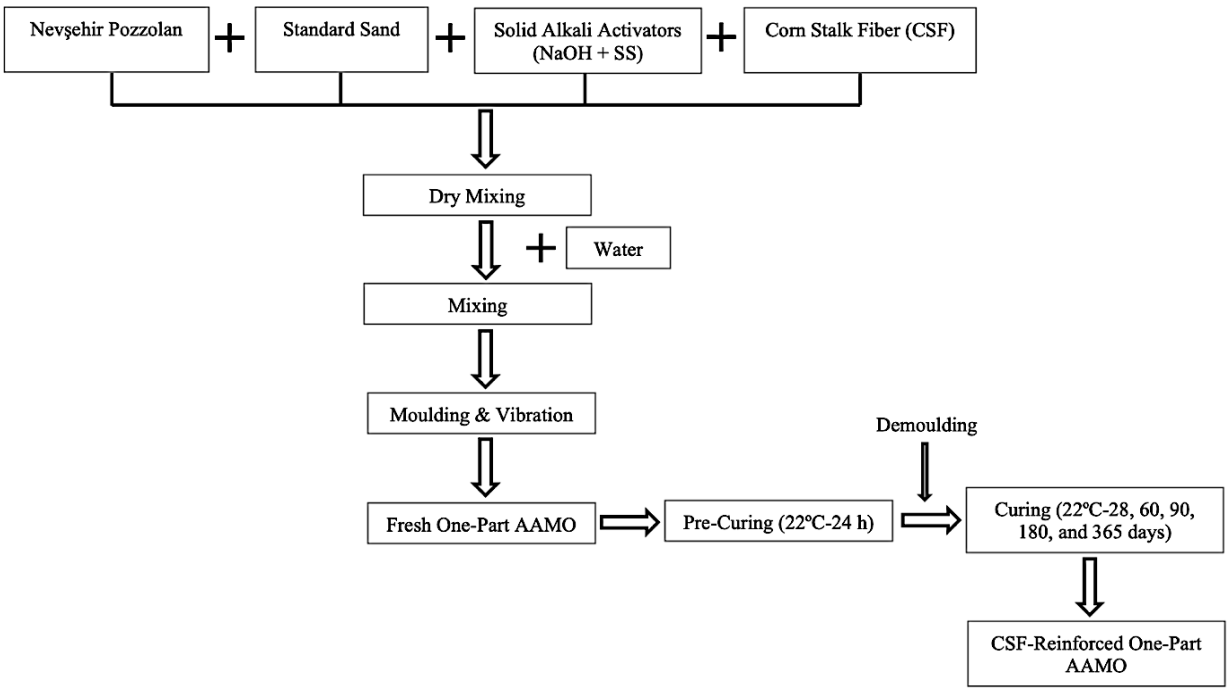

Fig. 3 Production stages of CSF-reinforced one-part AAMO samples

To determine the physical properties such as UW, WA, and P, the weights of the samples in dry and water-saturated conditions, as well as those suspended in water, were measured. The dry sample weight (m_d) was obtained by drying the samples at 100±2 °C for approximately 36 hours. Afterwards, the same samples were maintained in a water-filled container for 48 hours to ascertain the water-saturated weight (m_s). The weight in water (m_h) of the samples is denoted when they are suspended in a water-filled container. The UW (g/cm^3) was calculated according to Equation 1 in accordance with TS EN 1015-10:

$$UW = \frac{m_d}{m_{s\text{-}m_h}} \quad (1)$$

The WA of the samples under atmospheric pressure was determined based on Equation 2 in accordance with TS EN 13755 [73]:

$$WA = \frac{m_s\text{-}m_d}{m_d} \times 100 \quad (2)$$

The specific weight is defined as the weight of the unit volume of the material in a void-free state. To calculate the P, the specific weight must be determined. The specific weight (ρ_r) is determined according to TS 699 [74] by finely grinding a certain amount of material into powder form, adding it to a water-filled glass bottle, and ensuring that the material completely settles at the bottom without any air bubbles. The specific weights of the samples were calculated according to Equation 3:

$$\rho_r = \frac{m_{kn} - m_k}{(m_{kn} - m_{k)} - (m_{kns} - m_{sd)}} \quad (3)$$

"m_k" is the weight of the empty bottle, "m_{kn}" is the weight of the bottle filled only with the sample, "m_{sd}" is the weight of the water-filled bottle, and "m_{kns}" is the weight of the water- and sample-filled bottle.

The P of the samples was calculated according to Equation 4:

$$P = (1\text{-}\frac{UW}{\rho_r}) \times 100 \quad (4)$$

The UPV was calculated using a Proceq device according to TS EN 14579. The device automatically detects the UPV by attaching probes to the samples' endpoints, and it processes the sample length (L, mm) into the database. When the device was operated, the time (t, μs) until the UPV provided by the transmitting probe was received by the receiving probe was determined, and the UPV (km/s) was calculated in accordance with the following Equation 5:

$$UPV = \frac{L}{t} \quad (5)$$

The MoE (GPa) of the samples, whose UW and UPV were determined separately, was calculated according to Equation 6:

$$MoE = \frac{UPV^2 \times UW \times 10^5}{g} \quad (6)$$

"g" represents the acceleration attributable to gravity, quantified as 9.81 m/s².

Dimensional variations of the materials, including swelling and shrinking, might have a negative impact on the materials' anticipated efficiency. More swelling might have a detrimental impact on the properties due to the development of interior microcracks in the structure. Therefore, in accordance with ISO 8335 [75], the thickness of swelling (ToS) of the fiber-reinforced materials submerged in a water-filled container for 24 hours ought to be less than 2%. The ToS was determined by using Equation 7:

$$ToS = (\frac{d_2 - d_1}{d_1}) \times 100 \quad (7)$$

"d_1" and "d_2" represent the thickness (mm) prior to and after immersion in the water-filled container, respectively.

The TC was calculated using a heat flux device under steady-state conditions in accordance with ASTM C518-17 [76]. The heat flow measurement device is comprised of two copper plates, a single heat flux transducer, and a protective shell with thermal insulation that prevents the loss of heat.

The heat flow through two copper plates was measured after the sample was placed between them. The sensors were used to measure the heat flux (Q, W/m^2), and the temperature differences between the copper plates ($\Delta T = T_1 - T_2$). TC (W/mK) was calculated using Equation 8:

$$Q = TC \times \frac{\Delta T}{d} \quad (8)$$

"d" denotes the thickness (m).

The FS and CS tests were conducted in accordance with TS EN 196-1 [67]. The FS (MPa) was calculated using Equation 9, and the CS (MPa) was calculated using Equation 10:

$$FS = \frac{1.5 \times F_f \times l}{b^3} \quad (9)$$

$$CS = \frac{F_c}{A} \quad (10)$$

"b" represents the width of the prismatic sample (mm), "F_f" is the maximum bending load (N), "l" denotes distances between two supports (mm), "F_c" is the maximum compressive load the sample receives (N), and "A" is the cross-sectional area of the sample (mm^2).

3. Results and Discussion

3.1. The Impact of CSF Incorporation on the Physical Performance of AAMO

The impacts of CSF content and length on the physical properties, such as P, WA, UW, and ToS of AAMO, are shown in Figure 4.

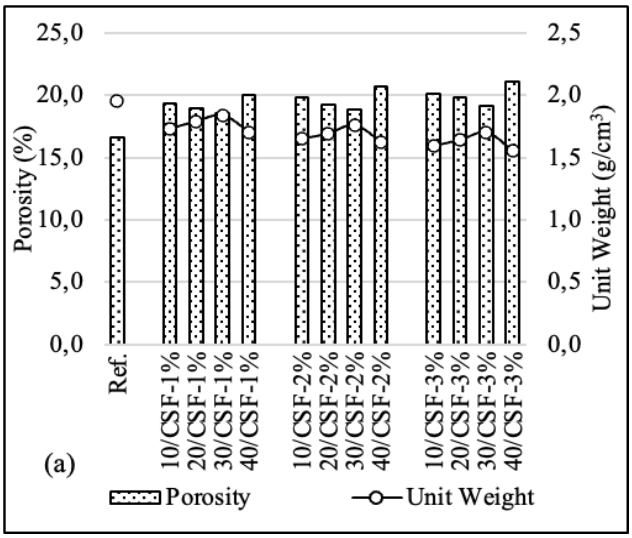

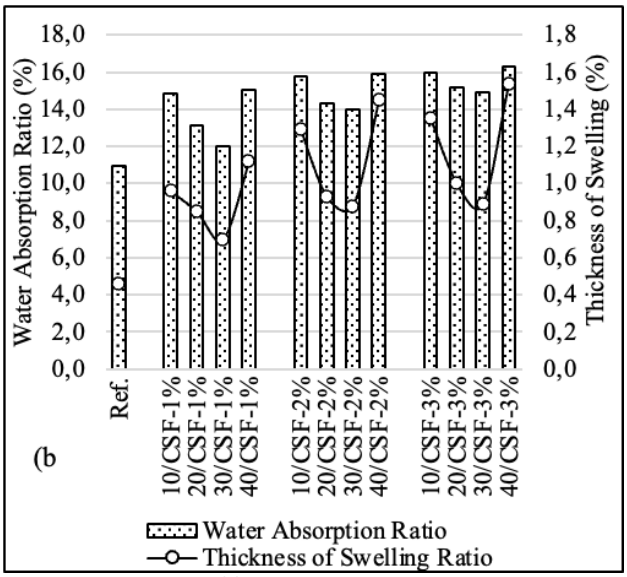

Fig. 4 The impacts of fiber content and length on the physical performance of AAMO: (a) P and UW relationship, and (b) WA and ToS relationship.

Incorporation of 1%, 2%, and 3% CSF by weight into AAMO gradually increased the P of the mortar while reducing its UW (Figure 4(a)). While the P of the reference sample was 16.61%, the addition of 1%, 2%, and 3% CSF increased it to ranges of 18.54-20.00%, 18.90-20.75%, and 19.11-21.13%, respectively. As expected from the increase in the P, the UW of the reference sample, which was 1.95 g/cm³, decreased to 1.70-1.84, 1.62-1.76, and 1.55-1.70 g/cm^3 with the addition of 1%, 2%, and 3% CSF, respectively. The increase in P detected with the increasing CSF content might be due to the porous internal structure of CSF. Another reason was that the CSF within the fresh matrix absorbed the mixing water and incorporated it into its structure. The absorbed water then evaporated as the mixture dried under ambient conditions, leaving behind entrapped air. Due to this entrapped air, the P increased [47]. This increasing trend in P had also been observed in the literature for AAMs based on coconut and sisal [41], cotton [44], and sugarcane bagasse [47]. The P of the one-part AAMO containing CSF (18.54-21.13%) was higher compared to the sugarcane bagasse-based AAMO (10-15%) [47], but lower compared to the cotton (22-26%) [44], coconut (26-29%), and sisal (27-30%)-based [41] AAMOs.

The WA of the reference mortar was the lowest (10.96%). The addition of CSF to the mortar, especially increasing the fiber content from 1% to 3%, increased the WA to a range of 12.01-16.33% (Figure 4(b)). This increase was parallel to the increase in P. The increase in WA was due to the matrix becoming more porous and the higher WA capacity of natural CSF due to its hydrophilic character. When water molecules contacted with the hydrophilic components of CSF, a considerable amount of hydrogen bonds were formed, creating a physical barrier between the fiber and the matrix, thereby reducing the adhesion at the fiber-matrix interface [77]. The natural fiber, which absorbed a large amount of water, swelled, leading to tensile stresses within the matrix and consequently causing micro-cracks to form. Thus, the fiber could be separated from the matrix [78, 79]. The effect of increased fiber content on enhancing WA was also identified in the literature in AAM based on coconut and sisal [41], hemp [43], and sugarcane bagasse [47].

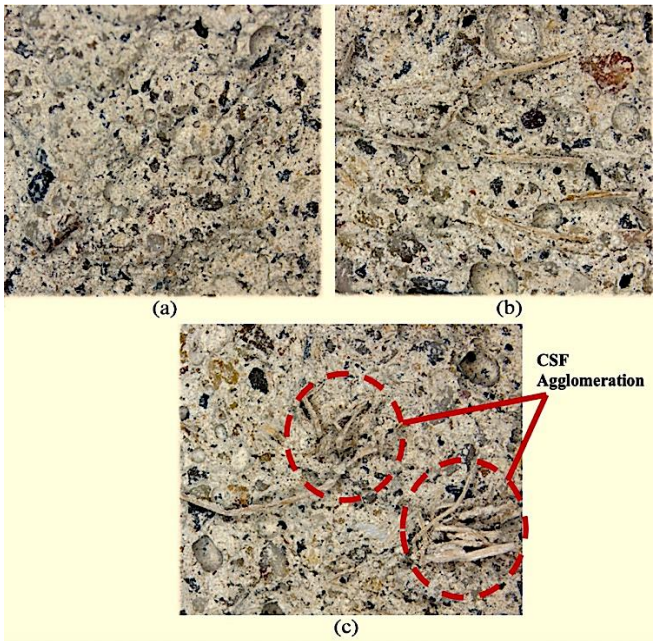

Fig. 5 Optical microscope images of the samples: (a) Reference sample without CSF, (b) Sample containing 3%-30 mm CSF, and (c) Agglomeration occurring in the sample containing 3%-40 mm CSF.

When the CSF content was kept constant, increasing the CSF length from 10 mm to 20 and 30 mm resulted in a gradual decrease in P and WA, while the UW increased. However, with the use of CSF longer than 30 mm, an opposite trend in physical properties was observed. Especially in samples with 40 mm CSF (3% fiber content), the highest P (21.13%), WA

(16.33%), and the lowest UW (1.55 g/cm^3) were observed, indicating that the critical CSF length (where the interaction between CSF and the matrix was maximized) was exceeded. This situation might be due to the tendency of fibers to clump more with the use of longer CSF. The mixing of the 40 mm CSF made it difficult to obtain a homogeneous matrix, leading to the concentration and agglomeration of CSF in certain areas within the mortar and the formation of gaps between the matrix and CSF. The observed agglomeration of fibers overlapped with the digital images of the samples detected by the optical microscope and is shown in Figure 5(c). In contrast, the reference sample had a homogeneous internal structure (Figure 5(a)), and in samples with a critical CSF length (30 mm), a more homogeneous fiber distribution was observed (Figure 5(b)).

High levels of swelling in water-absorbing materials can negatively affect the mechanical properties due to the development of micro-cracks in the structure [78]. Therefore, swelling of the fiber-reinforced materials should be less than 2% [75]. As seen in Figure 4(b), the lowest ToS (0.46%) was obtained in the reference sample. As the length and content of CSF increased, the ToS exhibited a rise between 0.70% and 1.54%. However, the low values identified are important in terms of meeting the expected requirements of the material.

3.2. The Impact of CSF Incorporation on the Thermal Performance of AAMO

The impacts of CSF content and length on the relationship between TC and P of AAMO are shown in Figure 6.

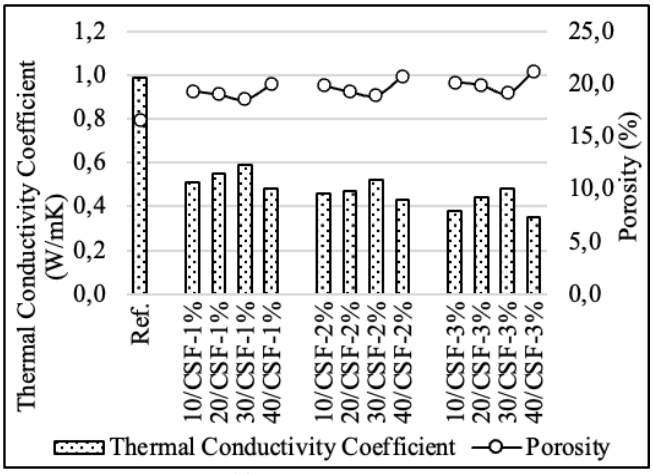

Fig. 6 The impacts of fiber content and length on the TC and P relationship of AAMO

The TC of the reference mortar was 0.99 W/mK. With CSF reinforcement, the TC gradually decreased to 0.35 W/mK. The TC of the samples was inversely related to their P. In other words, the increased P resulting from the incorporation of CSF into AAMO meant that a greater number of pores within the material served as thermal insulation [80]. This conclusion is because the air trapped within the larger number of voids in AAMO had a TC (0.025 W/mK) that was lower than that of the matrix, generally ranging from 1.0 to 1.2 W/mK. By increasing the CSF content to 3%, the larger amount of CSF created a more porous internal structure, which further reduced the TC of the material. The effect of fiber length on the TC also varied inversely with the change in P. Up to a fiber length of 30 mm, the TC showed an increasing trend, while for fiber lengths exceeding 30 mm, the TC decreased because of the formation of a more porous internal structure and the tendency of CSF to clump together. In this study, the sample with the lowest TC (0.35 W/mK) was determined to be coded 40/CSF-%3. In the literature, the TC of AAMO reinforced with 7.5% sugarcane bagasse fiber by weight was 0.55 W/mK [81], AAMO containing 1% sisal fiber was 0.98 W/mK, and AAMO containing 1% coconut fiber was 0.94 W/mK [41]. In this study, the TC of AAMO containing 1%, 2%, and 3% CSF (0.48-0.59 W/mK, 0.43-0.52 W/mK, and 0.35-0.48 W/mK, respectively) was lower than the values identified in the literature, indicating that CSF enabled the production of AAMO with improved thermal performance.

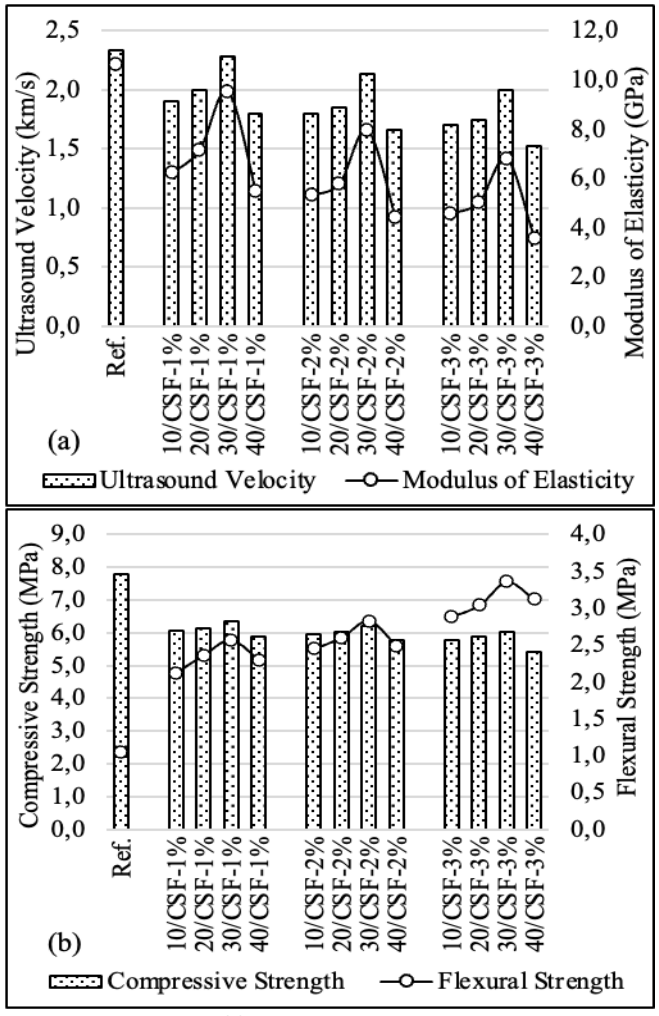

Fig. 7 The impacts of fiber content and length on the mechanical performance of AAMO: (a) UPV and MoE, and (b) CS and FS relationship.

3.3. The Impact of CSF Incorporation on the Mechanical Performance of AAMO

The impacts of CSF content and length on the mechanical properties, such as UPV, MoE, FS, and CS of AAMO are shown in Figure 7. The highest UPV (2.34 km/s) belonged to the reference sample. The reduction of UPV to 1.52 km/s with the addition of CSF was another indication of the higher P of the samples containing CSF. The change in the UPV, with CSF content and length, was inversely proportional to the change in P. Additionally, a directly proportional relationship was identified between the material's FS, CS, and the UPV. When the CSF content was increased to 3% and the CSF length was extended to 30 mm, the UPV increased. In 40-mm CSF-incorporated samples, the highest P, caused by more agglomeration of the fibers, resulted in the lowest UPV. The MoE is the resistance of AAMO to deformation under load. The highest MoE (10.67 GPa) was obtained from the reference sample and gradually decreased with an increase in CSF content up to 3% and an increase in fiber length beyond 30 mm. The rising trend of the MoE values was related directly to the decrease of the P and the increase of the UW.

The lowest FS (1.05 MPa) was detected in the reference sample without CSF. Reinforcing AAMO with 1% CSF increased the FS by 2.02-2.45 times compared to the reference sample. Increasing the CSF content to 2% and 3% increased the FS by 2.33-2.70 times and 2.75-3.20 times, respectively. The enhanced tensile strength of the CSF, coupled with the significant adhesion between the matrix and CSF, facilitates the transmission of loads from the matrix to the CSF [41]. Additionally, the increase in FS indicated that CSF could act as a bridge between cracks, thereby preventing further crack propagation. Because when a crack comes into contact with CSF, the higher energy is necessary to remove the CSF from the matrix, overcome adhesion, and cause the crack to propagate across the matrix. This bridging effect of CSF prevents sudden fracture by distributing the stress between various parts of the material. When stresses again exceed the material's capacity in other regions, more cracks appear, and the process is repeated [82]. This finding is important as it aligns with the findings of existing literature that show that sisal [40, 41], coconut [41], jute [40], cotton [44, 45], musa basjoo [52], and lignin [83] fibers significantly increase the FS of AAMO.

With the increase in CSF length from 10 mm to 20 and 30 mm, the FS increased in all fiber contents. The increased strength up to a 30 mm CSF length could be ascribed to the interfacial adhesion between the matrix and CSF. Shorter fibers provide friction due to a higher number of fiber ends, while longer fibers offer higher deformation resistance [86]. The highest FS at 1%, 2%, and 3% CSF contents (2.57, 2.83, and 3.36 MPa, respectively) were observed in samples with a fiber length of 30 mm. This finding was consistent with physical property results. Therefore, the critical fiber length required for the production of a higher-strength CSF-reinforced one-part AAMO was 30 mm. On the other hand, increasing the CSF length to 40 mm led to a decrease in FS. This was because the presence of longer fibers within the matrix led to fiber agglomeration and the formation of weaker interfacial regions. However, the FS of the samples with 40 mm CSF was higher than both the reference sample and the samples with 10 mm CSF.

The highest CS (7.80 MPa) was found in the reference sample. In the samples reinforced with 1% CSF, the CS decreased to the range of 5.90-6.34 MPa. In contrast, in the samples reinforced with 2% and 3% CSF, it decreased to 5.77-6.19 MPa and 5.42-6.03 MPa, respectively. In other words, adding more CSF to the one-part AAMO negatively affected the development of CS. Increasing the CSF length from 10 mm to 20 and 30 mm positively affected the development of CS. In the samples reinforced with 1%, 2%, and 3% CSF, the highest CS was observed in the 30 mm fiber length, with values of 6.34 MPa, 6.19 MPa, and 6.03 MPa, respectively. This result was important as it was aligned with the development of physical properties. The lowest CS (5.42 MPa) was found in the AAMO with the highest ratio and the longest CSF (40/CSF-%3). This finding was consistent with other research results as well [47, 81, 87]. The decrease in strength when the fiber content and fiber length exceed critical values was due to the formation of weaker regions within the matrix, resulting from the increased P of the mortar, as well as the insufficient bridging of potential cracks in the matrix by fibers [52]. However, the purpose of adding CSF to one-part AAMO is not to increase the CS of the material but to enhance ductility and prevent brittle fracture. Therefore, the aforementioned CS losses could be negligible. The CS obtained from the one-part AAMO reinforced with CSF (5.42-6.34 MPa) was higher than that of the 1% lignin-based AAMO (3.5 MPa) [83], but lower than that of the AAMO containing 2% jute or 3% sisal (20.6 and 22.1 MPa, respectively) [84] and the AAMO containing 0.25-1.5% musa basjoo fibers (45-50 MPa) [52].

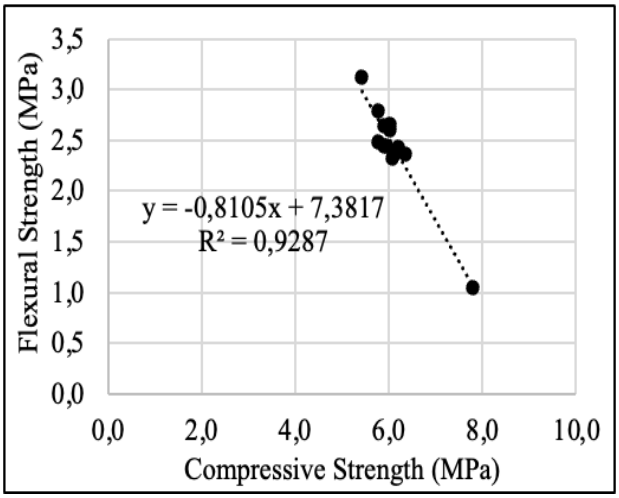

Fig. 8 Relationship between CS and FS

The relationship between CS and FS for all samples is presented in Figure 8. The CS varied inversely with the increase in FS. The CSF incorporation reduced the CS of one-part AAMO while increasing its FS. It was observed that the points were concentrated on a line. Additionally, the FS and CS showed a strong linear relationship with a correlation coefficient of 0.9287.

3.4. The Impact of CSF Incorporation on the Fracture Behaviour of AAMO

The impacts of CSF content and length on the flexural load and displacement relationship of AAMO are shown in Figure 9. During the initial loading, a linear elastic deformation was observed. As the load increased, microcracks developed within the material, indicating the formation of a nonlinear deformation curve. In all samples reinforced with CSF, the peak loads and the area under the stress-strain curve were higher than those of the reference sample. The sudden decrease of the curve after reaching the peak load in the reference sample indicated that a brittle fracture occurred. Additionally, the reference sample completely fractured under load and separated into two pieces (Figure 10(a)).

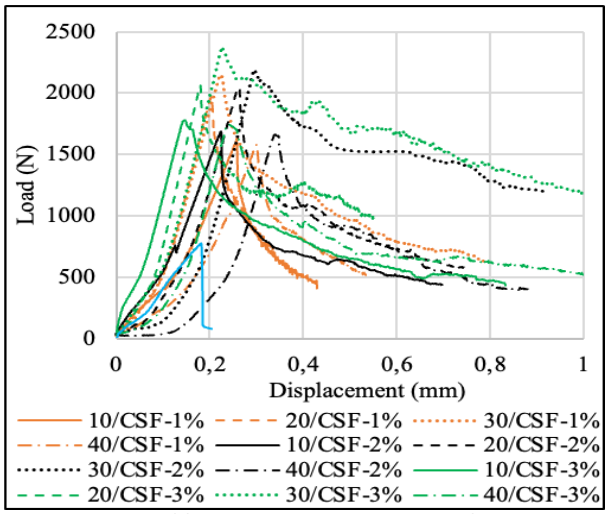

Fig. 9 The impacts of fiber content and length on the flexural load and displacement relationship of AAMO

CSF showed significant effectiveness in the fracture behavior of one-part AAMO. Unlike the reference sample, which exhibited brittle fracture behavior, the CSF-reinforced samples showed significant deformation under load and a large area under the stress-strain curve, indicating the development of ductile fracture behavior and high energy absorption capacity. Thus, the material showed signs of fracture before it completely broke (Figure 10(b)). With the increase in CSF content from 1% to 3%, the toughness of CSF-reinforced AAMO increased further. In samples with a higher fiber content, although matrix fragmentation occurred after the initial crack formation, the CSF prevented the complete breaking of the matrix, thus maintaining sample integrity (Figure 10(c)).

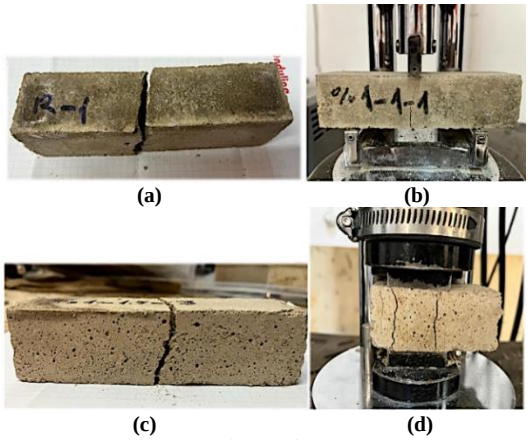

Fig. 10 (a) Brittle fracture of the reference sample and complete separation of the pieces from each other, (b) Crack propagation is slow and fracture behaviour is ductile in the CSF-reinforced samples, (c) Although the matrix breaks, the CSF prevents complete separation and holds the matrix together, and (d) Deformation of the CSF-reinforced samples before fracture under the effect of compression loads.

CSF-reinforced samples did not exhibit sudden and brittle fracture behavior during the test, showing significant deformations before fragmentation (Figure 10(d)). Maintaining the integrity of the material was particularly important for preventing serious injuries to users, especially under the influence of significant horizontal forces such as an earthquake, until they could escape the building. The increase in CSF length from 10 mm to 30 mm positively enhanced the toughness. However, the lower toughness value detected in samples with 40 mm CSF might be due to the agglomeration of fibers within the matrix, leading to void formation and weakening adhesion between the CSF and the matrix. In this case, CSF could be insufficient in preventing crack propagation.

3.5. The Impact of Curing Period on the Performance of AAMO

Curing is the process applied to maintain the required temperature and humidity conditions during the period when the physical, mechanical, and durability properties of a fresh binding material develop. When the material is subjected to ideal curing conditions in the early stage, it becomes volumetrically stable, impermeable, and possesses high strength and abrasion resistance, along with increased durability against aging agents that may develop over time [87]. AAM is generally cured under ambient conditions, by the heat effect in an oven, the heat and steam effect in an autoclave, and the microwave effect. In curing methods based on heat energy consumption, the heat acts as an activator for the development of alkali activation reactions, resulting in the final material generally having relatively high mechanical properties [88, 89]. However, heating leads to high energy consumption during the application. Curing under ambient conditions, without consuming any heat energy, is a more economical and environmentally friendly option.

After determining the optimum CSF content by weight as 3% and the CSF length as 30 mm, which provides the highest physical and mechanical properties for the one-part AAMO, the changes in the physical and mechanical properties with increasing curing period up to 365 days are presented in Figures 11 and 12, respectively.

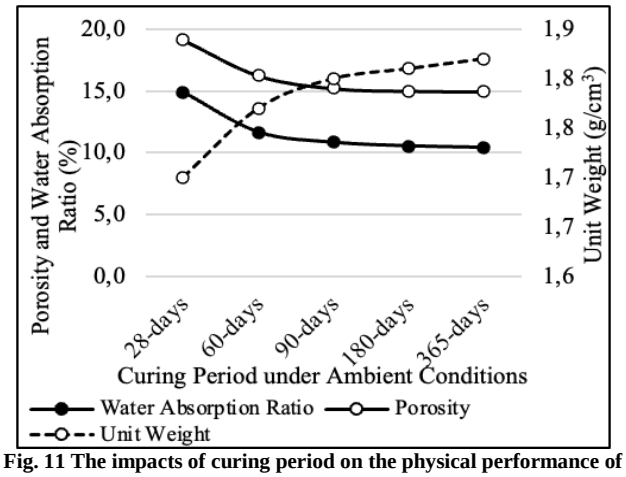

Fig. 11 The impacts of curing period on the physical performance of AAMO

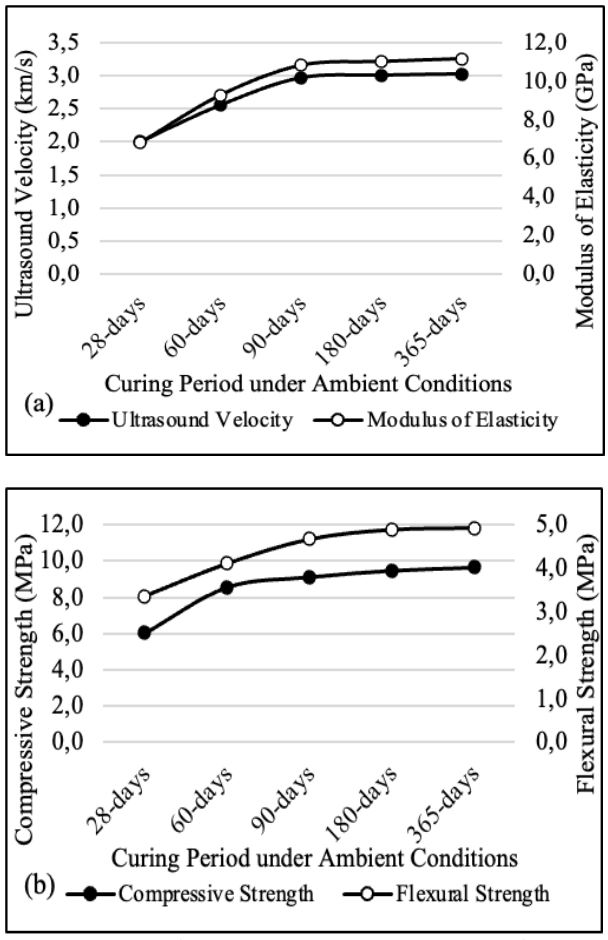

Fig. 12 The impacts of curing period on the mechanical performance of AAMO: (a) UPV and MoE relationship, and (b) CS and FS relationship.

As the curing period under laboratory conditions of 22±2°C and 50±5% RH increased from 28 days to 60 and 90 days, the UW of the 30/CSF-%3 sample increased, while the values of P and WA gradually decreased. This positive development observed in the physical properties indicated that the internal structure of the material was continuing to evolve. As expected, the properties of the mortar, such as UPV, MoE, FS, and CS, continued to increase. A study in the literature reported that the FS of metakaolin-based AAM reinforced with coir fiber and cured under ambient conditions for 20 months increased by 12%. It could be emphasized that the natural fiber could maintain its performance over time, without losing its effectiveness under high alkaline conditions, as indicated by the aforementioned increase [77]. In this context, the increase in the mechanical properties of the CSF-reinforced one-part AAMO after 12 months was consistent with the literature. However, after the first 90 days, the rate of increase in properties tended to slow down. It was determined that the curve between 180 and 365 days approached horizontal. From this, it could be inferred that the effectiveness of AAMO in internal structure development was high in the first 90 days, and increasing the curing period beyond 90 days did not lead to further improvement in the properties.

In terms of sustainability, the use of CSF in AAMO may provide several environmental advantages. Corn stalks are produced in substantial quantities as agricultural waste during maize harvesting. In many parts of Türkiye, these wastes are often thrown away by burning them in the open or letting them break down naturally. This can make the air dirty and release more greenhouse gases. Using CSF in the production of wall materials, therefore, represents a value-added approach to managing agricultural waste while supporting circular resource management. Compared with commonly used synthetic fibers, including polypropylene, polyvinyl alcohol, and glass, CSF generally requires significantly less energy during processing. Since the manufacturing of synthetic fibers is typically associated with high energy consumption and considerable carbon emissions, replacing synthetic fibers with CSF may help lower the environmental impact of the produced materials. Although a comprehensive life cycle assessment study was not carried out in the context of the current study, the use of CSF in AAMO can still be regarded as a promising approach for improving the sustainability of AAMO while also promoting the management of agricultural residues.

From a practical perspective, the use of CSF in AAMO could provide promising opportunities for large-scale production and potential field applications. One-part AAMOs are particularly attractive because they simplify the preparation process. In these systems, the dry constituents are mixed and then activated by adding water, just like conventional cement-based materials. Such an approach not only makes the wall material easier to handle but also

improves convenience during storage, transportation, and on-site use. In addition, utilizing waste CSF can help reduce the overall material cost while simultaneously offering an alternative pathway for managing agricultural waste. Despite these encouraging observations, further investigation is still necessary, particularly with regard to long-term durability and the feasibility of large-scale production. However, the results of this study indicate that CSF-reinforced AAMOs could be a good choice for creating more eco-friendly wall materials.

Considering the optimal CS (5.42-6.34 MPa) and lower UW (1.55-1.84 g/cm^3) ranges, the produced CSF-reinforced one-part AAMOs are suitable for the production of non-load bearing wall materials and prefabricated components in the construction sector. The existence of CSF enhances the resistance to cracking and toughness, which may be beneficial for the dimensional stability of the produced material. However, future research needs to determine the long-term effectiveness and durability of the CSF-reinforced one-part AAMO against various aging agents.

4. Conclusion

The results of the current experimental research conducted to produce CSF-reinforced one-part AAMO can be summarized as follows:

- CSF is a natural fiber from waste that may be used to increase the physical and mechanical properties of one-part AAMO and to prevent its brittle fracture behaviour.
- The CSF content and length are primary parameters that exert a considerable influence on the evolution of the material properties.
- Gradually increasing the fiber content (up to 3%, by weight) increases the P and WA of AAMO and decreases the UW, UPV, MoE, and CS. The increase in FS in parallel with the increase in fiber content demonstrates that CSF has effective adhesion to the matrix and is successful in bridging the formed cracks to prevent crack propagation.
- Increasing CSF content results in a reduction of TC, enhancing thermal insulation properties of the AAMO.
- The critical CSF length that allows for the development of the highest properties was determined to be 30 mm. Using longer fibers, fiber agglomeration occurs in certain areas within the matrix, and a porous structure forms around these fiber clumps. Therefore, when longer fibers are used, the properties of the AAMO decrease.
- The fracture behaviour of AAMO without CSF is sudden and brittle, whereas the addition of CSF results in a more ductile fracture behaviour with higher toughness. For the production of one-part AAMO with higher mechanical properties and resistance to crack propagation, the optimum CSF content and length were determined as 3% and 30 mm, respectively.
- Extending the curing period from 28 to 365 days positively influenced the characteristics of the mortar. However, the efficacy of the curing period is higher, especially in the first 90 days, while it is negligible in improving material properties between 90 and 365 days.
- By using CSF in the production of AAMO, a solution has been found for the waste problem after corn harvesting, and an alternative to the use of synthetic-based fibers produced by consuming energy has been developed. Additionally, it has aided in the prevention of the CO_2 emissions resulting from the burning of waste corn stalks.
- Changes in the physical, mechanical, and thermal properties of CSF-reinforced one-part AAMO over a 365-day curing period were identified in the current study. The long-term durability of the AAMO against various aging agents needs to be determined in future research. Freezing-thawing, wetting-drying, sulphate attack, and resistance to high temperatures are among the primary parameters that need to be investigated. In addition, the environmental impact of the produced AAMO should be determined by performing a comprehensive life cycle assessment analysis.
- In this study, CSF-reinforced one-part AAMO was produced with dimensions of 40x40x160 mm in accordance with the available laboratory facilities. Whether this material can be used to produce wall panels, which are widely used in the construction sector, and to determine the effectiveness of the fibers on mechanical properties needs to be examined in further study by manufacturing them in the dimensions of commercially available wall panels.

References

[1] Qingwen Xue, Zhaojun Wang, and Qingyan Chen, "Multi-Objective Optimization of Building Design for Life Cycle Cost and CO_2 Emissions: A Case Study of a Low-Energy Residential Building in a Severe Cold Climate," *Building Simulation*, vol. 15, no. 1, pp. 83-98, 2021. [CrossRef] [Google Scholar] [Publisher Link]

[2] Bassam A. Tayeh et al., "Durability and Mechanical Properties of Cement Concrete Comprising Pozzolanic Materials with Alkali-Activated Binder: A Comprehensive Review," *Case Studies in Construction Materials*, vol. 17, pp. 1-17, 2022. [CrossRef] [Google Scholar] [Publisher Link]

[3] Bree Bennett, Phillip Visintin, and Tianyu Xie, "Global Warming Potential of Recycled Aggregate Concrete with Supplementary Cementitious Materials," *Journal of Building Engineering*, vol. 52, 2022. [CrossRef] [Google Scholar] [Publisher Link]

[4] B. Cantero et al., "Durability of Concretes Bearing Construction and Demolition Waste as Cement and Coarse Aggregate Substitutes," *Cement and Concrete Composites*, vol. 134, 2022. [CrossRef] [Google Scholar] [Publisher Link]

[5] Ahmad L. Almutairi et al., "Potential Applications of Geopolymer Concrete in Construction: A Review," *Case Studies in Construction Materials*, vol. 15, pp. 1-20, 2021. [CrossRef] [Google Scholar] [Publisher Link]

[6] Joseph Davidovits, "Properties of Geopolymer Cements," *First International Conference on Alkaline Cements and Concretes*, KIEV Ukrain, vol. 1, pp. 131-149, 1994. [Google Scholar]

[7] Riccardo Maddalena, Jennifer J. Roberts, and Andrea Hamilton, "Can Portland Cement Be Replaced by Low-Carbon Alternative Materials? A Study on The Thermal Properties and Carbon Emissions of Innovative Cements," *Journal of Cleanear Production*, vol. 186, pp. 933-942, 2018. [CrossRef] [Google Scholar] [Publisher Link]

[8] Yanguang Wu et al., "Geopolymer, Green Alkali Activated Cementitious Material: Synthesis, Applications and Challenges," *Construction and Building Materials*, vol. 224, pp. 930-949, 2019. [CrossRef] [Google Scholar] [Publisher Link]

[9] Bassam A. Tayeh et al., "Effect of Elevated Temperatures on Mechanical Properties of Lightweight Geopolymer Concrete," *Case Studies in Construction Materials*, vol. 15, pp. 1-21, 2021. [CrossRef] [Google Scholar] [Publisher Link]

[10] Ali Allahverdi, Kamyar Mehrpour, and Ebrahim Najafi Kani, "Investigating the Possibility of Utilizing Pumice-Type Natural Pozzonal in Production of Geopolymer Cement," *Ceramics Silicates*, vol. 52, no. 1, pp. 16-23, 2008. [Google Scholar] [Publisher Link]

[11] Dali Bondar et al., "Effect of Type, Form, and Dosage of Activators on Strength of Alkali-Activated Natural Pozzolans," *Cement and Concrete Composites*, vol. 33, no. 2, pp. 251-260, 2011. [CrossRef] [Google Scholar] [Publisher Link]

[12] Mostafa Vafaei, and Ali Allahverdi, "Influence of Calcium Aluminate Cement on Geopolymerization of Natural Pozzolan," *Construction and Building Materials*, vol. 114, pp. 290-296, 2016. [CrossRef] [Google Scholar] [Publisher Link]

[13] Claudio Finocchiaro et al., "FT-IR Study of Early Stages of Alkali Activated Materials based on Pyroclastic Deposits (Mt. Etna, Sicily, Italy) Using Two Different Alkaline Solutions," *Construction and Building Materials*, vol. 262, pp. 1-11, 2020. [CrossRef] [Google Scholar] [Publisher Link]

[14] Roberta Occhipint et al., "Alkali Activated Materials using Pumice from The Aeolian Islands (Sicily, Italy) and their Potentiality for Cultural Heritage Applications: Preliminary Study," *Construction and Building Materials*, vol. 259, 2020. [CrossRef] [Google Scholar] [Publisher Link]

[15] Germana Barone et al., "Potentiality of the use of Pyroclastic Volcanic Residues in the Production of Alkali Activated Material," *Waste and Biomass Valorization*, vol. 12, no. 2, pp. 1075-1094, 2020. [CrossRef] [Google Scholar] [Publisher Link]

[16] Patrick N. Lemougna, Kenneth J.D. MacKenzie, and U.F. Chinje Melo, "Synthesis and Thermal Properties of Inorganic Polymers (Geopolymers) for Structural and Refractory Applications from Volcanic Ash," *Ceramics International*, vol. 37, no. 8, pp. 3011-3018, 2011. [CrossRef] [Google Scholar] [Publisher Link]

[17] Hervé Kouamo Tchakouté et al., "Utilization of Volcanic Ashes for The Production of Geopolymers Cured at Ambient Temperature," *Cement and Concrete Composites*, vol. 38, pp. 75-81, 2013. [CrossRef] [Google Scholar] [Publisher Link]

[18] B.I. Djon Li Ndjock, Antoine Elimbi, and Martin Cyr, "Rational Utilization of Volcanic Ashes based on Factors Affecting their Alkaline Activation," *Journal of Non-Crystalline Solids*, vol. 463, pp. 31-39, 2017. [CrossRef] [Google Scholar] [Publisher Link]

[19] Juhyuk Moon et al., "Characterization of Natural Pozzolan-based Geopolymeric Binders," *Cement and Concrete Composites*, vol. 53, pp. 97-104, 2014. [CrossRef] [Google Scholar] [Publisher Link]

[20] Mohammed Ibrahim et al., "Influence of Nano-SiO_2 on the Strength and Microstructure of Natural Pozzolan based Alkali Activated Concrete," *Construction and Building Materials*, vol. 173, pp. 573-585, 2018. [CrossRef] [Google Scholar] [Publisher Link]

[21] Rami H. Haddad, and Zainab K. Lababneh, "Geopolymer Composites using Natural Pozzolan and Oil-Shale Ash base Materials: A Parametric Study," *Construction and Building Materials*, vol. 240, 2020. [CrossRef] [Google Scholar] [Publisher Link]

[22] Hayami Takeda et al., "Fabrication and Characterization of Hardened Bodies from Japanese Volcanic Ash using Geopolymerization," *Ceramics International*, vol. 40, no. 3, pp. 4071-4076, 2014. [CrossRef] [Google Scholar] [Publisher Link]

[23] Dongping Song et al., "Feasibility Exploration on The Geopolymerization Activation of Volcanic Tuff, Parametrical Optimization, and Reaction Mechanisms," *Journal of Materials Research and Technology*, vol. 11, pp. 618-632, 2021. [CrossRef] [Google Scholar] [Publisher Link]

[24] D.J. Ilham et al., "The Potential use of Volcanic Deposits for Geopolymer Materials," *IOP Conference Series Earth and Environmental Science*, vol. 497, no. 1, pp. 1-9, 2020. [CrossRef] [Google Scholar] [Publisher Link]

[25] Rafia Firdous, and Dietmar Stephan, "Impact of The Mineralogical Composition of Natural Pozzolan on Properties of Resultant Geopolymers," *Journal of Sustainable Cement-based Materials*, vol. 10, no. 3, pp. 149-164, 2021. [CrossRef] [Google Scholar] [Publisher Link]

[26] Rafael Robayo-Salazar et al., "Alkali-Activated Binary Mortar based on Natural Volcanic Pozzolan for Repair Applications," *Journal of Building Engineering*, vol. 25, 2019. [CrossRef] [Google Scholar] [Publisher Link]

[27] Mehrzad Mohabbi Yadollahi, Ahmet Benli, and Ramazan Demirboğa, "The Effects of Silica Modulus and Aging on Compressive Strength of Pumice-based Geopolymer Composites," *Construction and Building Materials*, vol. 94, pp. 767-774, 2015. [CrossRef] [Google Scholar] [Publisher Link]

[28] S.T. Erdoğan, "Inexpensive Intumescent Alkali-Activated Natural Pozzolan Pastes," *Journal of the European Ceramic Society*, vol. 35, no. 9, pp. 2663-2670, 2015. [CrossRef] [Google Scholar] [Publisher Link]

[29] Refika Çetintaş, and Sezen Soyer-Uzun, "Relations between Structural Characteristics and Compressive Strength in Volcanic Ash based One-Part Geopolymer Systems," *Journal of Building Engineering*, vol. 20, pp. 130-136, 2018. [CrossRef] [Google Scholar] [Publisher Link]

[30] Ilker Tekin, "Properties of NaOH Activated Geopolymer with Marble, Travertine and Volcanic Tuff Wastes," *Construction and Building Materials*, vol. 127, pp. 607-617, 2016. [CrossRef] [Google Scholar] [Publisher Link]

[31] E. Yaşar, and Y. Erdoğan, "Evaluation of Acidic (Nevşehir) and Basic (Osmaniye) Pumice in the Construction Sector," *Proceedings of the Türkiye International Mining Congress and Fair*, Turky, pp. 409-418, 2005. [Google Scholar]

[32] Fatih Kantarcı, İbrahim Türkmen, and Enes Ekinci, "Optimization of Production Parameters of Geopolymer Mortar and Concrete: A Comprehensive Experimental Study," *Construction and Building Materials*, vol. 228, 2019. [CrossRef] [Google Scholar] [Publisher Link]

[33] Serife Ozata, Busra Akturk, and Nabi Yuzer, "Utilization of Waste Cappadocia Earth as a Natural Pozzolan in Alkali Activation: A Parametric Study," *Construction and Building Materials*, vol. 329, 2022. [CrossRef] [Google Scholar] [Publisher Link]

[34] Muhammad Riaz Ahmad et al., "Multiproperty Characterization of Cleaner and Energy-Efficient Vegetal Concrete based on One-Part Geopolymer Binder," *Journal of Cleaner Production*, vol. 253, 2020. [CrossRef] [Google Scholar] [Publisher Link]

[35] Hai-Yan Zhang, Jian-Cheng Liu, and Bo Wu, "Mechanical Properties and Reaction Mechanism of One-Part Geopolymer Mortars," *Construction and Building Materials*, vol. 273, 2021. [CrossRef] [Google Scholar] [Publisher Link]

[36] Cong Ma et al., "Properties and Characterization of Green One-Part Geopolymer Activated by Composite Activators," *Journal of Cleaner Production*, vol. 220, pp. 188-199, 2019. [CrossRef] [Google Scholar] [Publisher Link]

[37] Sajjad Yousefi Oderji et al., "Fresh and Hardened Properties of One-Part Fly Ash-based Geopolymer Binders Cured at Room Temperature: Effect of Slag and Alkali Activators," *Journal of Cleaner Production*, vol. 225, pp. 1-10, 2019. [CrossRef] [Google Scholar] [Publisher Link]

[38] Yi Wang, Hui Zhong, and Mingzhong Zhang, "Experimental Study on Static and Dynamic Properties of Fly Ash-Slag based Strain Hardening Geopolymer Composites," *Cement and Concrete Composites*, vol. 129, pp. 1-15, 2022. [CrossRef] [Google Scholar] [Publisher Link]

[39] Azizatul Karimah et al., "A Review on Natural Fibers for Development of Eco-Friendly Bio-Composite: Characteristics, and Utilizations," *Journal of Materials Research and Technology*, vol. 13, pp. 2442-2458, 2021. [CrossRef] [Google Scholar] [Publisher Link]

[40] Guido Silva et al., "Optimization of A Reinforced Geopolymer Composite using Natural Fibers and Construction Wastes," *Construction and Building Materials*, vol. 258, 2020. [CrossRef] [Google Scholar] [Publisher Link]

[41] Ampol Wongsa et al., "Natural Fiber Reinforced High Calcium Fly Ash Geopolymer Mortar," *Construction and Building Materials*, vol. 241, 2020. [CrossRef] [Google Scholar] [Publisher Link]

[42] Oguzhan Yavuz Bayraktar et al., "Hemp Fiber Reinforced One-Part Alkali-Activated Composites with Expanded Perlite: Mechanical Properties, Microstructure Analysis and High-Temperature Resistance," *Construction and Building Materials*, vol. 363, 2023. [CrossRef] [Google Scholar] [Publisher Link]

[43] Bojan Poletanovic et al., "Physical and Mechanical Properties of Hemp Fibre Reinforced Alkali-Activated Fly Ash and Fly Ash/Slag Mortars," *Construction and Building Materials*, vol. 259, 2020. [CrossRef] [Google Scholar] [Publisher Link]

[44] Thamer Salman Alomayri, and I.M. Low, "Synthesis and Characterization of Mechanical Properties in Cotton Fiber-Reinforced Geopolymer Composites," *Journal of Asian Ceramic Societies*, vol. 1, no. 1, pp. 30-34, 2013. [CrossRef] [Google Scholar] [Publisher Link]

[45] Thamer Salman Alomayri, Faiz Uddin Ahmed Uddin Ahmed Shaikh, and I.M. Low, "Characterisation of Cotton Fibre-Reinforced Geopolymer Composites," *Composites Part B-Engineering*, vol. 50, pp. 1-6, 2013. [CrossRef] [Google Scholar] [Publisher Link]

[46] G. Silva et al., "Evaluation of Fire, High-Temperature and Water Erosion Resistance of Fiber-Reinforced Lightweight Pozzolana-based Geopolymer Mortars," *IOP Conference Series: Materials Science and Engineering*, vol. 706, no. 1, pp. 1-8, 2019. [CrossRef] [Google Scholar] [Publisher Link]

[47] Rachel Nkwaju Yanou et al., "Performance of Laterite-Based Geopolymers Reinforced with Sugarcane Bagasse Fibers," *Case Studies in Construction Materials*, vol. 15, pp. 1-16, 2021. [CrossRef] [Google Scholar] [Publisher Link]

[48] Al-Ghazali Noor Abbas et al., "Effects of Fibers Length on the Properties of Kenaf Fibers-Reinforced Geopolymer Concrete," *AIP Conference Proceedings*, vol. 2447, no. 1, 2021. [CrossRef] [Google Scholar] [Publisher Link]

[49] Na Zhang et al., "Effects of Alkali-Treated Kenaf Fiber on Environmentally Friendly Geopolymer-Kenaf Composites: Black Liquid as the Regenerated Activator of the Geopolymer," *Construction and Building Materials*, vol. 297, 2021. [CrossRef] [Google Scholar] [Publisher Link]

[50] Georgy Lazorenko et al., "Effect of Pre-Treatment of Flax Tows on Mechanical Properties and Microstructure of Natural Fiber Reinforced Geopolymer Composites," *Environmental Technology and Innovation*, vol. 20, 2020. [CrossRef] [Google Scholar] [Publisher Link]

[51] G. Silva et al., "A Comparative Study of Linen (Flax) Fibers as Reinforcement of Fly Ash and Clay Brick Powder based Geopolymers," *IOP Conference Series: Materials Science and Engineering*, vol. 416, pp. 1-8, 2018. [CrossRef] [Google Scholar] [Publisher Link]

[52] Yeddula Bharath Simha Reddy, S. Praburanganathan, and Minakshi Mishra, "Experimental Investigation on the Fiber Reinforced Ash-based Geopolymer Concrete with Musa Basjoo Fibers," *Materials Today: Proceedings*, vol. 65, no. 8, pp. 3700-3706, 2022. [CrossRef] [Google Scholar] [Publisher Link]

[53] Hanzhou Ye et al., "Interfacial Bonding Properties of the Eco-Friendly Geopolymer-Wood Composites: Influences of Embedded Wood Depth, Wood Surface Roughness, and Moisture Conditions," *Journal of Materials Science*, vol. 56, no. 12, pp. 7420-7433, 2021. [CrossRef] [Google Scholar] [Publisher Link]

[54] K. Taşdan, *Egypt Situation and Forecast Report*, 1st ed., Ankara, Türkiye: TEPGE Publishing, 2023. [Publisher Link]

[55] Monireh Fattahi et al., "Waste Corn Husk Fibers for Sound Absorption and Thermal Insulation Applications: A Step towards Sustainable Buildings," *Journal of Building Engineering*, vol. 77, pp. 1-12, 2023. [CrossRef] [Google Scholar] [Publisher Link]

[56] Peihan Wang et al., "Study on Preparation and Performance of Alkali-Activated Low Carbon Recycled Concrete: Corn Cob Biomass Aggregate," *Journal of Materials Research and Technology*, vol. 23, pp. 90-105, 2023. [CrossRef] [Google Scholar] [Publisher Link]

[57] Solomon Oyebisi et al., "Evaluation of Reactivity Indexes and Durability Properties of Slag-based Geopolymer Concrete Incorporating Corn Cob Ash," *Construction and Building Materials*, vol. 258, pp. 1-15, 2020. [CrossRef] [Google Scholar] [Publisher Link]

[58] Saloni et al., "Performance of Rice Husk Ash-based Sustainable Geopolymer Concrete with Ultra-Fine Slag and Corn Cob Ash," *Construction and Building Materials*, vol. 279, pp. 1-37, 2021. [CrossRef] [Google Scholar] [Publisher Link]

[59] Luiz Arthur Silva de Aquino et al., "Agro-Industrial Waste from Corn Straw Fiber: Perspectives of Application in Mortars for Coating and Laying Blocks based on Ordinary Portland Cement and Hydrated Lime," *Construction and Building Materials*, vol. 353, 2022. [CrossRef] [Google Scholar] [Publisher Link]

[60] Haochen Wang et al., "Influence of the use of Corn Straw Fibers to Connect the Interfacial Transition Zone with the Mechanical Properties of Cemented Coal Gangue Backfill," *Construction and Building Materials*, vol. 367, 2023. [CrossRef] [Google Scholar] [Publisher Link]

[61] Rachid Kidari, and Amine Tilioua, "Investigation of the Thermomechanical Characteristics of Compressed Earth Bricks Reinforced with Cement and Corn Straw Waste Fibers," *Cleaner Waste Systems*, vol. 9, pp. 1-14, 2024. [CrossRef] [Google Scholar] [Publisher Link]

[62] Zheng Wu, Xiuli Wang, and Zhihua Chen, "Experimental Study on Preparation and Performance of the Corn Straw Fiber (CSF) Reinforced EPS Concrete," *Journal of Building Engineering*, vol. 89, 2024. [CrossRef] [Google Scholar] [Publisher Link]

[63] Zhipeng Jin et al., "Pre-Treated Corn Straw Fiber for Fiber-Reinforced Concrete Preparation with High Resistance to Chloride Ions Corrosion," *Case Studies in Construction Materials*, vol. 19, pp. 1-16, 2023. [CrossRef] [Google Scholar] [Publisher Link]

[64] Sean S. Musil, P.F. Keane, and W.M. Kriven, "Green Composite: Sodium-based Geopolymer Reinforced with Chemically Extracted Corn Husk Fibers," *Developments in Strategic Materials and Computational Design IV*, vol. 34, pp. 123-133, 2014. [CrossRef] [Google Scholar] [Publisher Link]

[65] TS EN 196-6 Data Sheet, Methods of Testing Cement-Part 1: Determination of Strength, European Committee for Standardization, Brussels, Turkish Standard Institution, Ankara, Türkiye, 1995. [Online]. Available: https://nazhco.com/wp-content/uploads/2021/04/bs_en_196_1_1995_methods_of_testing_cement_part_1_determination_of_strength.pdf

[66] I. Garcia-Lodeiro, A. Palomo, and A. Fernández-Jiménez, *2-An Overview of The Chemistry of Alkali-Activated Cement-based Binders*, Handbook of Alkali-Activated Cements, Mortars and Concretes, pp. 19-47, 2015. [CrossRef] [Google Scholar] [Publisher Link]

[67] TS EN 196-1 Data Sheet, Turkish Standard Institution, Ankara, Türkiye. [Online]. Available: https://standards.globalspec.com/std/10228279/ts-en-196-1

[68] Mazed M. Kabir et al., "Chemical Treatments on Plant-based Natural Fibre Reinforced Polymer Composites: An Overview," *Composites Part B: Engineering*, vol. 43, no. 7, pp. 2883-2892, 2012. [CrossRef] [Google Scholar] [Publisher Link]

[69] Mazed M. Kabir et al., "Tensile Properties of Chemically Treated Hemp Fibres as Reinforcement for Composites," *Composites Part B: Engineering*, vol. 53, pp. 362-368, 2013. [CrossRef] [Google Scholar] [Publisher Link]

[70] Geon-Wook Lee, and Young-Cheol Choi, "Effect of Abaca Natural Fiber on the Setting Behavior and Autogenous Shrinkage of Cement Composite," *Journal of Building Engineering*, vol. 56, 2022. [CrossRef] [Google Scholar] [Publisher Link]

[71] Xiaoli Xie et al., "Influence of Pretreatment of Rice Straw on Hydration of Straw Fiber Filled Cement based Composites," *Construction and Building Materials*, vol. 113, pp. 449-455, 2016. [CrossRef] [Google Scholar] [Publisher Link]

[72] TS EN 12350-5 Data Sheet, Turkish Standard Institution, Ankara, Türkiye. [Online]. Available: https://standards.globalspec.com/std/10238757/ts-en-12350-5

[73] TS EN 13755 Data Sheet, Turkish Standard Institution, Ankara, Türkiye. [Online]. Available: https://standards.globalspec.com/std/10233625/ts-en-13755

[74] TS 699 Data Sheet, Turkish Standard Institution, Ankara, Türkiye. [Online]. Available: https://www.alldatasheet.com/view_datasheet.jsp?Searchword=TS699

[75] ISO 8335 Data Sheet, International Organization for Standardization, UK, 1987. [Online]. Available: https://www.iso.org/obp/ui#iso:std:iso:8335:ed-1:v1:en

[76] ASTM C518-17 Data Sheet, Standard Test Method for Steady-State Thermal Transmission Properties by Means of the Heat Flow Meter Apparatus ASTM International, West Conshohocken, USA, 2021. [Online]. Available: https://store.astm.org/c0518-17.html

[77] Marfa Molano Camargo et al., "A Review on Natural Fiber-Reinforced Geopolymer and Cement-based Composites," *Materials*, vol. 13, no. 20, pp. 1-29, 2020. [CrossRef] [Google Scholar] [Publisher Link]

[78] T. Alomayri et al., "Effect of Water Absorption on the Mechanical Properties of Cotton Fabric-Reinforced Geopolymer Composites," *Journal of Asian Ceramic Societies*, vol. 2, no. 3, pp. 223-230, 2014. [CrossRef] [Google Scholar] [Publisher Link]

[79] Hongyan Chen, Menghe Miao, and Xin Ding, "Influence of Moisture Absorption on the Interfacial Strength of Bamboo/Vinyl Ester Composites," *Composites Part A: Applied Science and Manufacturing*, vol. 40, no. 12, pp. 2013-2019, 2009. [CrossRef] [Google Scholar] [Publisher Link]

[80] E. Prud'homme, E. Joussein, and S. Rossignol, *26 - Alkali-Activated Concrete Binders as Inorganic Thermal Insulator Materials*, Handbook of Alkali-Activated Cements, Mortars and Concretes, England: Woodhead Publishing Limited, pp. 687-728, 2015. [CrossRef] [Google Scholar] [Publisher Link]

[81] R.Y. Nkwaju et al., "Iron-Rich Laterite-Bagasse Fibers based Geopolymer Composite: Mechanical, Durability and Insulating Properties," *Applied Clay Science*, vol. 183, pp. 1-10, 2019. [CrossRef] [Google Scholar] [Publisher Link]

[82] Afonso R.G. de Azevedo et al., "Natural Fibers as an Alternative to Synthetic Fibers in Reinforcement of Geopolymer Matrices: A Comparative Review," *Polymers*, vol. 13, no. 15, 2021. [Google Scholar] [Publisher Link]

[83] Zhihao Su et al., "Influence of Different Fibers on Properties of Thermal Insulation Composites based on Geopolymer Blended with Glazed Hollow Bead," *Construction and Building Materials*, vol. 203, pp. 525-540, 2019. [CrossRef] [Google Scholar] [Publisher Link]

[84] Guido Silva et al., "Natural Fibers as Reinforcement Additives for Geopolymers - A Review of Potential Eco-Friendly Applications to the Construction Industry," *Sustainable Materials and Technologies*, vol. 23, pp. 1-11, 2020. [CrossRef] [Google Scholar] [Publisher Link]

[85] Kinga Korniejenko et al., "Mechanical Properties of Geopolymer Composites Reinforced with Natural Fibers," *Procedia Engineering*, vol. 151, pp. 388-393, 2016. [CrossRef] [Google Scholar] [Publisher Link]

[86] Tiesong Lin et al., "Effects of Fiber Length on Mechanical Properties and Fracture Behavior of Short Carbon Fiber Reinforced Geopolymer Matrix Composites," *Materials Science and Engineering: A*, vol. 497, no. 1-2, pp. 181-185, 2008. [CrossRef] [Google Scholar] [Publisher Link]

[87] Yash Nahata, Nirav Kholia, and T.G. Tank, "Effect of Curing Methods on Efficiency of Curing of Cement Mortar," *APCBEE Procedia*, vol. 9, pp. 222-229, 2014. [CrossRef] [Google Scholar] [Publisher Link]

[88] V.S. Athira et al., "Influence of Different Curing Methods on Mechanical and Durability Properties of Alkali Activated Binders," *Construction and Building Materials*, vol. 299, 2021. [CrossRef] [Google Scholar] [Publisher Link]

[89] M.S. Muñiz-Villarreal et al., "The Effect of Temperature on The Geopolymerization Process of a Metakaolin-based Geopolymer," *Materials Letters*, vol. 65, no. 6, pp. 995-998, 2011. [CrossRef] [Google Scholar] [Publisher Link]